

Polarization Change Monitor Based on Geometrical Analysis in Stokes Space

Jingnan Li⁽¹⁾, Yangyang Fan⁽¹⁾, Zhenning Tao⁽¹⁾, Hisao Nakashima⁽²⁾, Takeshi Hoshida⁽²⁾

⁽¹⁾ Fujitsu R&D Center, No. 8 Jian Guo Men Wai Ave., Beijing, China, lijingnan@fujitsu.com

⁽²⁾ Fujitsu Ltd., 1-1 Shin-ogura, Saiwai-Ku, Kawasaki 212-8510, Japan

Abstract We propose a novel polarization change monitor by analyzing geometrical relation of pilot symbols in Stokes space. The proposed monitor is experimentally verified and result shows that the polarization change in the range of quasi static to 3MHz can be captured.

Introduction

In optical fiber communication system, polarization change monitor has many applications. The fiber events, such as bending and shaking, can be detected by analyzing the state of polarization (SOP) change speed and pattern^[1]. The step size for tap-weight update in adaptive equalizer (AEQ) can be optimized based on the monitored polarization change speed. The polarization monitor could even be used for earthquake and tsunami detections^[2]. In reality, the polarization change speed spans over a wide range. In the case of mechanical vibration, it achieves several tens of kHz, defined as rotations per second in Stokes space^[3]. In the case of lightning strike, it is in the order of MHz^[4]. Consequently, a polarization change monitor needs to cover a wide frequency range.

Conventional polarization change monitor relies on the analyzing of AEQ tap-weights^{[1],[5]}. Those methods have a fundamental assumption that the AEQ realizes the inverse transfer function of the fiber link. However, this basic assumption is not always satisfied. Simple adaptation algorithms such as constant modulus algorithm (CMA) cannot track transient 1MHz polarization change caused by lightning strike. Therefore, the monitoring range of CMA based monitor is limited. Besides, CMA ignores the phase change in two polarization tributaries^[6]. As a result, polarization retarder of the link cannot be monitored by CMA based monitor and the monitored result becomes wrong^[7]. To overcome this problem, a monitor with joint processing of CMA and carrier phase recovery (CPR) is proposed^[7], but such joint processing has many engineering challenges in the real-time hardware design.

In this paper, we propose a novel polarization change monitoring method. By geometrically analyzing the SOP change of the pilot symbol (PS) in Stokes space, the rotation axis and rotation angle can be estimated. Then, the polarization change matrix and speed are calculated out. It does not depend on the unreliable assumption in conventional

method^{[1],[5]} and can be implemented by real-time digital signal processing (DSP)^[8]. Experimental results show that the polarization change from 10kHz to 1MHz can be monitored with 7% relative error and the transient polarization change up to 3MHz can also be captured.

Principle of proposed monitor

At transmitter (Tx) side, the SOPs of dual-polarization (DP) quadrature phase shift keying (QPSK) PSs are 4 points at $[0, 1, 0]$, $[0, 0, 1]$, $[0, -1, 0]$ and $[0, 0, -1]$ in Stokes space. In transmission, the polarization rotation and amplified spontaneous emission (ASE) noise cause SOP change and scattering, respectively. At receiver (Rx) side, the SOPs of DP-QPSK PSs are demonstrated in Fig. 1(a).

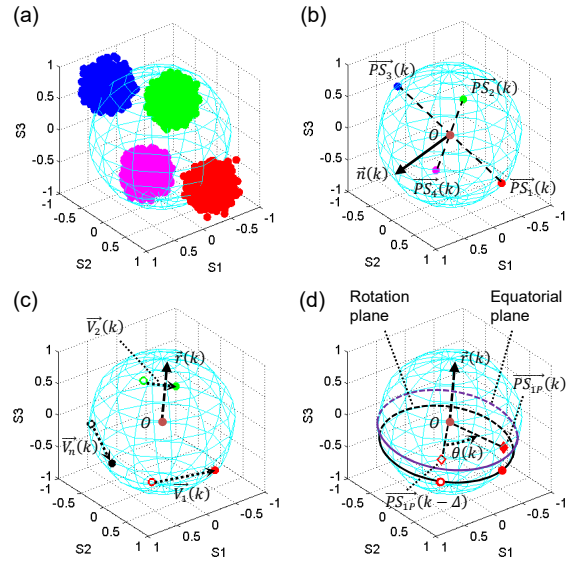


Fig. 1: Schematic of polarization change estimation in Stokes space. (a) Received SOPs, (b) averaged SOPs and normal vector estimation, (c) rotation axis estimation and (d) rotation angle estimation.

To eliminate the impact of ASE noise, the received PSs are firstly classified to 4-category and then averaged for each category. The averaged SOPs $\overline{PS}_1(k)$, $\overline{PS}_2(k)$, $\overline{PS}_3(k)$ and $\overline{PS}_4(k)$ are shown in Fig. 1(b), where k is the PS index. The normal vector of plane of averaged SOPs $\vec{n}(k)$ is obtained by cross product of the

two adjacent averaged SOPs, e.g., $\overrightarrow{PS_1}(k) \times \overrightarrow{PS_2}(k)$.

Next, the polarization change vectors $\overrightarrow{V_1}(k)$, $\overrightarrow{V_2}(k)$ and $\overrightarrow{V_n}(k)$ are obtained by calculating the difference of present and previous averaged SOPs (solid and hollow circles) $\overrightarrow{PS_1}(k) - \overrightarrow{PS_1}(k - \Delta)$, $\overrightarrow{PS_2}(k) - \overrightarrow{PS_2}(k - \Delta)$ and $\overrightarrow{n}(k) - \overrightarrow{n}(k - \Delta)$ as shown in Fig. 1(c), respectively, where Δ is the index difference between present and previous PSs. Those three vectors are all orthogonal to the rotation axis naturally. Thus, the rotation axis $\vec{r}(k)$ could be estimated by the cross product of any two polarization change vectors. To avoid the estimation error, the rotation axis $\vec{r}(k)$ with largest modulus is used.

After that, a pair of averaged SOPs, which polarization change vector has largest modulus, are used to estimate rotation angle, e.g., $\overrightarrow{PS_1}(k)$ and $\overrightarrow{PS_1}(k - \Delta)$. We define the rotation plane that is orthogonal to the rotation axis $\vec{r}(k)$ and contain the $\overrightarrow{PS_1}(k)$ and $\overrightarrow{PS_1}(k - \Delta)$. These averaged SOPs are projected onto the equatorial plane (assuming the rotation axis $\vec{r}(k)$ points toward north pole) by simply geometrical operation, then we have the projection vectors $\overrightarrow{PS_{1P}}(k)$ and $\overrightarrow{PS_{1P}}(k - \Delta)$ (solid and hollow diamonds) as shown in Fig. 1(d). The angle $\theta(k)$ between two projection vectors is the rotation angle and can be easily obtained based on geometrical relation.

According to rotation axis $\vec{r}(k)$ and rotation angle $\theta(k)$, the matrix of polarization change is described by

$$U(k) = \cos\left(\frac{\theta(k)}{2}\right) \mathbf{I} - j \sin\left(\frac{\theta(k)}{2}\right) \left(\frac{\vec{r}(k)}{|\vec{r}(k)|} \cdot \boldsymbol{\sigma}\right) \quad (1)$$

where \mathbf{I} and $\boldsymbol{\sigma}$ are identity and Pauli matrices, respectively. The speed of polarization change is calculated by

$$f(k) = \frac{|\theta(k)| \cdot B \cdot R}{2\pi \cdot \Delta} = \frac{|\theta(k)| \cdot PCR}{2\pi} \quad (2)$$

where B is symbol rate, R is PS insertion ratio and PCR is polarization calculation rate. It should be noted that the monitored result is updated for each PS index k .

Experimental setup

The experimental setup is demonstrated in Fig. 2. The 32GBaud DP-16 quadrature amplitude modulation (QAM) Nyquist signal with roll-off factor of 0.15 is used as transmitted signal. The DP-QPSK PS is periodically inserted into transmitted signal with the insertion ratio of 1/32. The dynamic polarization change is generated by a versatile polarization control platform (New Ridge Technologies, NRT-2500), which has spinner and randomizer modes to implement polarization changes with constant rotation rate

and random slew speed, respectively. The pre and post polarization controllers (PCs) are used to achieve static polarization change and control the rotation axis of dynamic polarization change. The 24dB optical signal-to-noise ratio (OSNR) is set by loading the lumped ASE noise. The input power of Rx is attenuated to -6dBm. After coherent detection, the baseband electrical signal is sampled at 80GSa/s. In Rx DSP, the data is firstly handled by Gram-Schmidt orthogonalization procedure to compensate the imperfection of Rx optical front end. Then, it is resampled to 2 samples per symbol and Rx skew is compensated. Next, pilot-aided 17-tap 2x2 CMA, frequency offset compensation and pilot-aided 4th-power CPR are used to recover transmitted signal. Notice that the proposed monitor is applied on the CMA input signal.

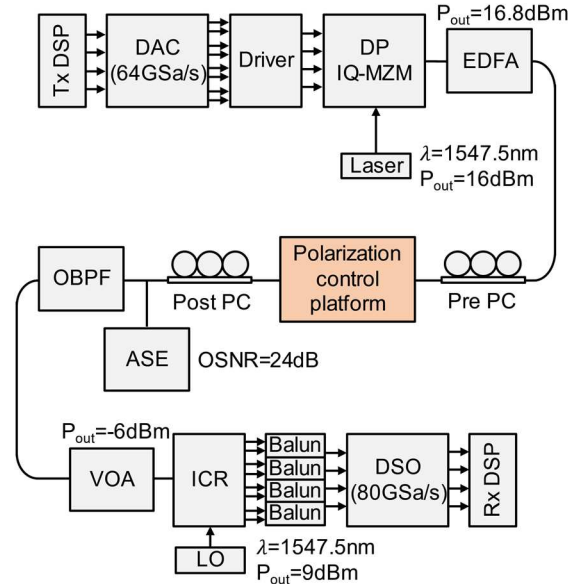


Fig. 2: Experimental setup. (DSP: digital signal processing; DAC: digital-to-analog converter; DP IQ-MZM: dual polarization in-phase/quadrature Mach-Zehnder modulator; EDFA: Erbium doped fiber amplifier; PC: polarization controller; OBPF: optical bandpass filter; ASE: amplified spontaneous emission; OSNR: optical signal-to-noise ratio; VOA: variable optical attenuator; ICR: integrated coherent receiver; LO: local oscillator; Balun: balanced to unbalanced transformer; DSO: digital storage oscilloscope)

Experimental results

We set the polarization control platform at spinner mode to generate polarization change with constant rotation rate. To reduce the ASE noise induced SOP scattering sufficiently, the average length of PS of proposed monitor is fixed at 201. The performances of proposed monitor, CMA&CPR based monitor^[7] and CMA based monitor^[5] from 10kHz to 1MHz are demonstrated in Fig. 3. The polarization calculation rate is accordingly increased from 40kHz to 4MHz. It is worth noting that due to the limitation of device that the maximum constant rotation rate is

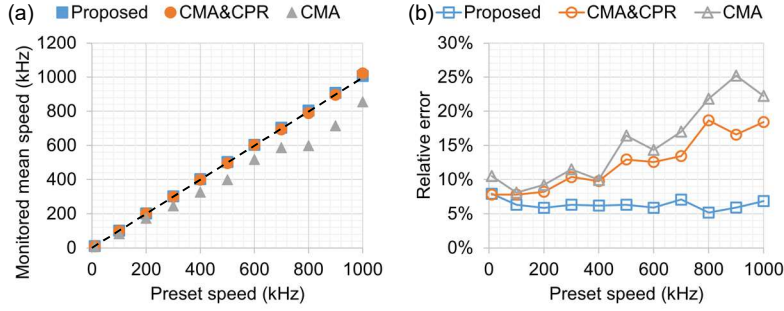


Fig. 3: Performance of three polarization change monitors. (a) Monitored mean speed and (b) relative error.

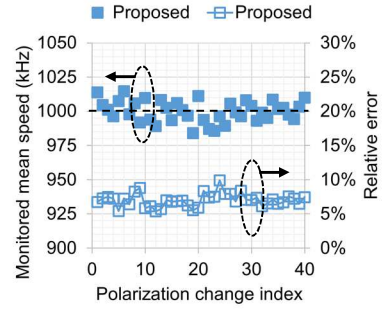


Fig. 4: Performance of proposed monitor at 1MHz polarization change.

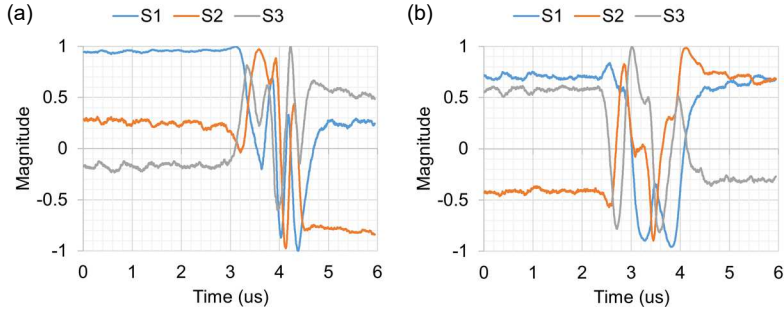


Fig. 5: Monitored Stokes parameters of normal vector in transient cases. (a) Case 1 and (b) case 2.

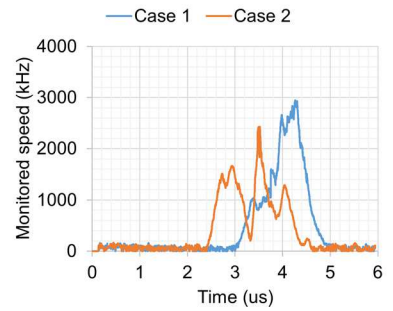


Fig. 6: Monitored real-time speeds of proposed monitor in transient cases.

100kHz, to evaluate the fast polarization change from 100kHz to 1MHz, the processing rate of Rx DSP is decreased from every 1 to every 10 PS. In Fig. 3(a), the monitored mean speeds of proposed monitor and CMA&CPR based monitor are close to preset values (black dashed line). But that of CMA based monitor are deviated from preset speed due to the neglect of polarization retarder. In Fig. 3(b), the relative error which is defined as the standard deviation of normalized error is independent with polarization change speed for the case of proposed method. Even at 1MHz, it is only 7%. However, as polarization change speed increasing, the relative error of other two monitors are increased and achieve about 20% at 1MHz. It is important to note that the step size of CMA and block size of CPR are optimized to achieve maximum Q factor for different polarization change speed. If they are not optimal, the monitored results of CMA&CPR based monitor and CMA based monitor are unreliable. Because the inverse transfer function of the fiber link cannot be estimated accurately, and the assumption is broken. By tuning two PCs, 40 polarization changes with fixed 1MHz rotation speed and different rotation axis are realized. In Fig. 4, the monitored mean values are nearly 1MHz (black dashed line) and the monitored relative error are mainly distributed in the range of 5% to 9%. Obviously, the proposed method can monitor as fast as 1MHz polarization change on whole Poincare sphere with stable performance.

Next, we set the polarization control platform at randomization mode to output the sudden and arbitrary polarization change and the random slow speed is more than 100kHz. The processing rate of Rx DSP is fixed at every 10 PS to emulate more than 1MHz random slow speed and the polarization calculation rate is fixed at 8MHz. The normal vector $\vec{n}(t)$, which has same SOP [1, 0, 0] with continuous-wave light at Tx side, is used to measure SOP transients and the monitored Stokes parameters of normal vector in two cases are shown in Fig. 5. Meanwhile, the monitored real-time speeds as shown in Fig. 6 demonstrate that the proposed method is effective to monitor transient polarization change from quasi static to 3MHz. Such ultra-wide monitoring range means it can be used to monitor transient polarization change caused by different fiber events such as mechanical vibration^[3] and lightning strike^[4].

Conclusions

A novel polarization change monitor is proposed in this paper. By analyzing the geometrical relation of PS in Stokes space, the polarization change can be estimated. Experimental results show that the polarization change with constant speed from 10kHz to 1MHz is monitored with 7% relative error and the transient polarization change from quasi static to 3MHz is captured. The proposed monitor provides a simple and effective way to monitor polarization status of fiber channel in practice.

References

- [1] F. Boitier *et al.*, "Proactive Fiber Damage Detection in Real-time Coherent Receiver", in *Proc. European Conference on Optical Communication*, Gothenburg, Sweden, Sep. 2017, Th.2.F.1.
- [2] M. Cantono *et al.*, "Sub-Hertz Spectral Analysis of Polarization of Light in a Transcontinental Submarine Cable", in *Proc. European Conference on Optical Communications*, Brussels, Belgium, Dec. 2020, Th2H-2.
- [3] P. M. Krummrich and K. Kotten, "Extremely fast (microsecond timescale) polarization changes in high speed long haul WDM transmission systems", in *Proc. Optical Fiber Communication Conference*, Los Angeles, United States, Feb. 2004, F13.
- [4] D. Charlton *et al.*, "Field measurements of SOP transients in OPGW, with time and location correlation to lightning strikes", *Opt. Express*, vol. 25, no. 9, pp. 9689–9696, 2017.
- [5] T. Ye *et al.*, "A polarization change monitor by eigenvalue analysis in coherent receiver", in *Proc. Optical Fiber Communication Conference*, San Diego, United States, Mar. 2019, M11.1.
- [6] K. Kikuchi, "Performance analyses of polarization demultiplexing based on constant-modulus algorithm in digital coherent optical receivers", *Opt. Express*, vol. 19, no. 10, pp. 9868-9880, 2011.
- [7] Y. Qi *et al.*, "Polarization Change Monitor Based on Jointly Applied Constant Modulus Algorithm and Carrier Phase Recovery in Coherent Receiver", in *Proc. Optoelectronics and Communications Conference and International Conference on Photonics in Switching and Computing*, Fukuoka, Japan, Jul. 2019, TuB2-4.
- [8] S. Okamoto *et al.*, "400 Gbit/s/ch field demonstration of modulation format adaptation based on pilot-aided OSNR estimation using real-time DSP", *IEICE Trans. Commun.*, vol. E100-B, no. 10, pp. 1726-1733, 2017.